


 Cite this: *RSC Adv.*, 2025, **15**, 16690

## Innovative eco-sustainable reishi mushroom-based adsorbents for progesterone removal and agricultural sustainability†

Abdalla Abdelwahab, <sup>a</sup> Khalaf M. Alenezi, <sup>a</sup> Jamal R. Humaidi, <sup>a</sup> Ashanul Haque, <sup>a</sup> Samar M. Mahgoub, <sup>b</sup> Aya M. Mokhtar, <sup>c</sup> Aya Shaban, <sup>d</sup> Mostafa Mansour M. M. <sup>e</sup> and Rehab Mahmoud <sup>\*f</sup>

The pervasive presence of endocrine-disrupting chemicals (EDCs), particularly progesterone, in aquatic ecosystems poses significant ecological and human health risks, necessitating the development of sustainable and efficient removal strategies. This study introduces an innovative, eco-friendly approach utilizing non-edible reishi mushroom (*Ganoderma lucidum*) and its calcined form as natural adsorbents for progesterone removal while simultaneously exploring the potential of the formed composites as sustainable agricultural amendments. The adsorption efficiency of both reishi mushroom powder and its calcined form was systematically optimized under varying pH, adsorbent dose, temperature, and contact time conditions. The adsorption capacities of reishi mushroom and its calcined form for progesterone were assessed using nine non-linear isotherm models. Among these, the Langmuir and Freundlich models provided the best fit to the experimental data ( $R^2 \sim 0.99$ ), demonstrating high adsorption capacities of  $90.52 \text{ mg g}^{-1}$  for reishi mushroom and  $118.10 \text{ mg g}^{-1}$  for calcined reishi mushroom under optimal conditions (pH 3, 25 °C, 0.1 g and 0.075 g doses, respectively) following pseudo-second-order and mixed-order kinetic models. Both materials were fully characterized before and after the adsorption process using XRD, FTIR, and SEM techniques. Thermodynamic analysis revealed the process to be exothermic, spontaneous, and highly ordered, driven by hydrophobic interactions and van der Waals forces. Molecular docking analysis shows that ganoderic acid A and progesterone bind strongly to key plant hormone receptors (GID1, TIR1, BRI1), indicating their potential to enhance plant growth by influencing gibberellin, auxin, and brassinosteroid signaling pathways. Beyond environmental remediation, the formed composites exhibited exceptional potential in enhancing agricultural productivity. Composite treatments, particularly progesterone adsorbed on calcined reishi mushroom, significantly improved seed germination rates (95%), shoot-to-root elongation (2.5 : 1), and overall plant growth (39 cm height, 200 g fresh weight). Soil quality assessments revealed increased organic matter content and improved fertility, highlighting the dual benefit of these adsorbents in environmental remediation and sustainable agriculture. The greenness profile of the proposed method, evaluated using NEMI, AGP, and Modified GAPI metrics, further underscores its eco-sustainability, with an eco-scale score of 94 and a BAGI blueness score of 75, affirming its alignment with green analytical chemistry principles. This study introduces a novel, cost-effective, and eco-friendly method for progesterone removal while pioneering the use of waste-derived adsorbents in circular agriculture. By utilizing reishi mushroom and its calcined form, this research addresses both water contamination and sustainable farming, advancing eco-friendly technologies.

Received 17th March 2025  
 Accepted 10th May 2025

DOI: 10.1039/d5ra01906k  
[rsc.li/rsc-advances](http://rsc.li/rsc-advances)

<sup>a</sup>Department of Chemistry, College of Sciences, University of Hail, Ha'il, 81451, Saudi Arabia. E-mail: [aabdelwahab@psas.bsu.edu.eg](mailto:aabdelwahab@psas.bsu.edu.eg); [k.alenezi@uoh.edu.sa](mailto:k.alenezi@uoh.edu.sa); [j.humaidi@uoh.edu.sa](mailto:j.humaidi@uoh.edu.sa); [a.haque@uoh.edu.sa](mailto:a.haque@uoh.edu.sa)

<sup>b</sup>Materials Science and Nanotechnology Department, Faculty of Postgraduate Studies for Advanced Sciences, Beni-Suef University, Egypt. E-mail: [miramar15@yahoo.com](mailto:miramar15@yahoo.com)

<sup>c</sup>Hydrology and Environment Department, Faculty of Earth Science, Beni-Suef University, 62511, Egypt. E-mail: [aya2451999mo@gmail.com](mailto:aya2451999mo@gmail.com)

<sup>d</sup>Faculty of Pharmacy, Cairo University, Egypt. E-mail: [ayaehuseani@gmail.com](mailto:ayaehuseani@gmail.com)

<sup>e</sup>Faculty of Agriculture, Department of Food Science and Technology, Al-Azhar University, Egypt. E-mail: [mostafamansour646@gmail.com](mailto:mostafamansour646@gmail.com)

<sup>f</sup>Chemistry Department, Faculty of Science, Beni-Suef University, Beni-Suef 62511, Egypt. E-mail: [rehabkhaled@science.bsu.edu.eg](mailto:rehabkhaled@science.bsu.edu.eg); Tel: +201111079459

† Electronic supplementary information (ESI) available. See DOI: <https://doi.org/10.1039/d5ra01906k>



## 1. Introduction

The presence of endocrine-disrupting chemicals (EDCs) in aquatic ecosystems has emerged as a global environmental concern, particularly due to their harmful effects on aquatic organisms and potential risks to human health. Among these contaminants is progesterone, primarily originating from pharmaceutical residues, wastewater treatment plants, and agricultural runoff, which poses significant ecological risks. When present in aquatic environments, progesterone can disrupt the endocrine systems of aquatic species, leading to altered reproductive behaviors, reduced fertility, and changes in species composition.<sup>1,2</sup> Given the widespread contamination of water bodies by hormonal pollutants, effective removal techniques are urgently needed to protect both the ecosystem and human health. Various methods have been explored for the removal of progesterone from water, including chemical degradation, membrane filtration, and photocatalysis. While these techniques have demonstrated some success, they often come with significant drawbacks, such as high operational costs, energy-intensive processes, and the generation of secondary pollutants.<sup>3-5</sup> Membrane filtration can also suffer from fouling and reduced efficiency, and photocatalysis often requires specific light conditions to be effective. In contrast, adsorption has gained recognition as a superior, cost-effective, and efficient method for the removal of organic contaminants like progesterone. The adsorption process relies on the ability of adsorbents to bind pollutants onto their surface, offering an easily scalable, energy-efficient, and sustainable alternative to other water treatment technologies.<sup>6,7</sup> The high surface area, pore volume, and ease of use make adsorption particularly attractive for removing progesterone and other steroid hormones from water. Among the various adsorbents explored, reishi mushroom (*Ganoderma lucidum*) stands out as a novel and promising material. Traditionally known for its medicinal properties, reishi mushroom has been found to possess excellent adsorption capacities due to its rich composition of polysaccharides, proteins, and other bioactive compounds.<sup>8,9</sup> This makes it a sustainable and biodegradable option for environmental remediation. Recent studies have highlighted the potential of reishi mushrooms to adsorb various organic pollutants, including progesterone, in a manner comparable to or even surpassing traditional adsorbents like activated carbon. On the other side, the calcination of reishi mushrooms enhances their adsorption properties, creating a promising material that combines the natural, renewable aspects of the mushroom with the high surface area and porosity of activated carbon.<sup>10</sup> Moreover, progesterone has been shown its ability to enhance plant growth, seed germination, and root and shoot elongation by mimicking auxin-like effects.<sup>11,12</sup> It promotes growth in plants like *Vigna radiata* and *Cucumis sativus* by influencing hormonal balance and gene activation.<sup>12,13</sup> However, progesterone's rapid degradation in soil limits its potential. In our study, we not only use reishi mushrooms (*Ganoderma lucidum*) and its calcinated form as natural adsorbents but also as controlled release systems in agriculture. These mushrooms can adsorb and gradually release progesterone, enhancing plant

growth.<sup>14</sup> Calcinated reishi mushroom derived from reishi further improves this effect due to its high surface area and porosity.<sup>15</sup> Green analytical chemistry focuses on minimizing environmental hazards, reducing costs, and promoting sustainability. Its principles emphasize using fewer solvents, low-toxicity chemicals, shorter analysis times, lower energy consumption, and developing user-friendly, integrated, and easily disassembled analytical instruments and methods.<sup>16</sup> Green chemistry metrics evaluate how well chemical processes align with sustainability principles, helping track performance improvements and assess environmental impact.<sup>17</sup> Several metrics have been developed to measure this alignment. The National Environmental Metrics Index (NEMI) provides a qualitative assessment,<sup>18</sup> while AGREE (Analytical GREENness Metric Approach and Software)<sup>19</sup> offers a quantitative evaluation. The Green Analytical Procedure Index (GAPI)<sup>18,20</sup> is semi-quantitative, and the recently introduced Blue Applicability Grade Index (BAGI) assesses the practicality and applicability ("blueness") of analytical techniques. These tools collectively advance greener and more efficient analytical practices.

In this study, we utilize reishi mushrooms (*Ganoderma lucidum*) and their calcined form as eco-friendly adsorbents for the removal of progesterone from aqueous media. We systematically investigate the adsorption behavior on both native powdered and thermally treated materials under varying conditions, while examining the adsorption kinetics and thermodynamic parameters to elucidate the underlying adsorption mechanisms. Furthermore, we explore the dual functionality of the formed composites as biofertilizers, assessing their impact on plant growth, seed germination, and root and shoot elongation. In addition, the study evaluates the environmental sustainability of the developed method using green chemistry metrics, reinforcing its potential for application in both environmental remediation and sustainable agriculture.

## 2. Experimental section

### 2.1. Materials and chemicals

Progesterone (with purity 99.87%) was purchased from Hubei Gedian Humanwell Pharmaceutical Co., Ltd (E-zhou City, Hubei, China), non-edible reishi mushrooms (*Ganoderma lucidum*) was obtained from Xi'an Herb Bio-Tech Co., Ltd (Xi'an, Shaanxi, China), Egyptian clover (*Trifolium alexandrinum*) were used for seed germination and growth experiments, distilled water, ethanol and Methanol were purchased from Merck (Darmstadt, Germany). HNO<sub>3</sub> and NaOH were obtained from Fisher Scientific, UK.

### 2.2. Preparation of powdered reishi mushroom (RM)

We used a vacuum oven to set it at the lowest temperature setting (40 °C) for 20 h to dry the mushrooms. Then, we used a high-powered blender to grind the dried reishi mushrooms, starting with small pieces and pulsing them into smaller chunks. Then, blend until they form a fine powder. Then, we stored the reishi mushroom powder in an airtight container and placed in a dark place to preserve its potency.



### 2.3. Preparation of calcinated RM (CRM)

The calcination process was performed by placing 10 g of the prepared dried mushrooms in a muffle furnace at 800 °C for 1 h. After calcination, the resulting material was cooled to room temperature and stored in a desiccator for further use.

### 2.4. Material characterization

Several analytical techniques were employed to characterize the prepared adsorbents and the formed composites, including X-ray diffraction (XRD), which utilized a PANalytical (Empyrean) instrument with Cu-K $\alpha$  radiation to assess sample crystallinity, scanning from 5° to 80° at 8° min $^{-1}$ . Fourier Transform Infrared Spectroscopy (FTIR) was conducted using a Bruker-Vertex 70 instrument *via* the KBr pellet technique, covering 400 to 4000 cm $^{-1}$ . The tested samples were examined by Scanning Electron Microscopy (SEM).

### 2.5. Preparation of standard solutions of progesterone

The concentrations of the samples were determined spectrophotometrically using a standard calibration curve. To select the analytical wavelength for the maximum absorbance method, a stock solution of progesterone was prepared by diluting progesterone in a mixture of methanol and water (80 : 20, v/v) to obtain a concentration of 1000  $\mu\text{g mL}^{-1}$ . Serial dilutions with different concentrations were then prepared from the stock solution using distilled water. The diluted solutions were scanned over a wavelength range of 200–400 nm using an Evolution 350 UV-Vis Spectrophotometer (Thermo Fisher Scientific, Massachusetts, USA) to quantify the progesterone content. The maximum absorbance wavelength ( $\lambda_{\text{max}}$ ) was recorded at 254 nm.<sup>21</sup>

### 2.6. Adsorption study

The experiment was conducted using a batch operating system at ambient temperature. A standard stock solution of PRG with a concentration of 1000  $\mu\text{g mL}^{-1}$  was prepared to facilitate the creation of a series of diluted concentrations for generating an ideal calibration curve (5–500  $\mu\text{g mL}^{-1}$ ). It was prepared by dissolving 50 mg of progesterone in 50 mL of a mixture of methanol and water (80 : 20, v/v), then the series of dilutions were prepared using distilled water.

**2.6.1. The effect of pH on the adsorption.** The effect of pH on the adsorption of progesterone onto both materials was investigated in the range of pH 3 to 9 as follow: in 50 mL Falcon tubes, we placed 0.05 g of each of dried reishi mushroom or calcinated reishi mushroom and PRG solution of 100  $\mu\text{g mL}^{-1}$  concentration. The pH of each solution was adjusted to 3–9 using 0.1 N NaOH or 0.1 N HCl, measured with a pH meter (Metrohm 751 Titroline), and then the tubes were placed on an orbital shaker (SO330-Pro). In another six tubes, the same procedure was repeated without adding the adsorbents. Before measurements, all prepared solutions were filtered using a syringe filter (Millipore, Nylon, 0.22  $\mu\text{m}$  pore size). The residual concentration of PRG in each solution was determined using an Evolution 350 UV-Vis Spectrophotometer at

a wavelength of 254 nm. The amount of PRG adsorbed per gram of either dried reishi mushroom or calcined reishi mushroom ( $Q_e$ ) and the removal percentage (%R) were calculated using the following equations:

$$Q_e = (C_0 - C_t)V/W \quad (1)$$

$$\%R = (C_0 - C_t) \times 100/C_0 \quad (2)$$

where,  $Q_e$ : is the amount of PRG adsorbed per gram of either dried reishi mushroom or calcined reishi mushroom;  $C_0$ ,  $C_t$  is the initial concentration and the concentration after adsorption of PRG in ( $\text{mg L}^{-1}$ ) at time  $t$  (min);  $W$ : the weight of dried reishi mushroom or its calcinated form in g and  $V$ : volume of PRG (L).

**2.6.2. Determination of the point of zero charge (pH<sub>pzc</sub>) of adsorbents.** The point of zero charge (pH<sub>pzc</sub>) of the adsorbents was determined using the pH drift method. In this procedure, a series of 50 mL NaCl solutions (0.01 M) were prepared in clean, closed containers. The initial pH (pH<sub>i</sub>) of each solution was adjusted to a range between 2 and 10 by adding either 0.1 N HCl or 0.1 N NaOH solutions, measured using a calibrated pH meter (Metrohm 751 Titroline). After adjusting the pH, 0.05 g of each adsorbent (dried reishi mushroom or calcinated reishi mushroom) was added to each solution. The suspensions were then shaken for 24 hours at room temperature using an orbital shaker (SO330-Pro) to reach equilibrium. Afterward, the final pH (pH<sub>f</sub>) of each solution was measured. The difference between the initial and final pH values ( $\Delta\text{pH} = \text{pH}_i - \text{pH}_f$ ) was plotted against the initial pH. The pH<sub>pzc</sub> was determined as the point where the curve crossed the line  $\Delta\text{pH} = 0$ .

**2.6.3. The effect of adsorbent dose on the adsorption.** The effect of adsorbent dose on the adsorption of progesterone onto both materials was investigated at a constant concentration of PRG (100  $\mu\text{g mL}^{-1}$ ) using various weights of each adsorbent (0.05 g to 0.30 g).

**2.6.4. Thermodynamics of the adsorption process.** The effect of temperature was examined at various temperatures: 25, 35, 45, and 55 °C, and the thermodynamic parameters were calculated.

**2.6.5. Determination of adsorption isotherms at different temperatures.** Non-linear isotherm models have been applied to investigate the effect of PRG concentration was studied at a constant weight of the adsorbent 0.1 g as an optimum condition of the dose of adsorbent for dried reishi mushroom and 0.075 g for calcinated reishi mushroom, applying different concentrations of PRG ranging from 5  $\mu\text{g mL}^{-1}$  to 500  $\mu\text{g mL}^{-1}$ .

**2.6.6. The effect of contact time and adsorption kinetic models.** The effect of contact time and adsorption kinetics of PRG onto the adsorbents had been studied using various kinetic models such as Pseudo-First-Order,<sup>22</sup> Pseudo-Second-Order,<sup>23</sup> intraparticle diffusion<sup>24</sup> and Avrami<sup>25</sup> at different time intervals ranging from 0 to 240 min.

### 2.7. Molecular docking study

In this study, docking simulations were conducted to evaluate the binding affinity of ganoderic acid A, a bioactive triterpenoid from *Ganoderma lucidum* (reishi mushroom) (1), and

progesterone, a steroid hormone known for its regulatory effects on growth and metabolism in various biological systems (2) to elucidate their potential in enhancing seed germination, plant growth, and elongation, supporting their application as biofertilizers.

To investigate this potential, three key plant hormone receptors were selected as molecular docking targets: GID1 (Gibberellin Receptor, PDB: 3ED1), which mediates gibberellin perception and signaling, regulating stem elongation, seed germination, and reproductive development (3). If ganoderic acid A or progesterone exhibit significant binding affinity to GID1, they may modulate gibberellin-related growth pathways, TIR1 (Auxin Receptor, PDB: 2P1Q) which is a crucial component of the auxin signaling pathway, controlling cell division, elongation, and organ development (4). Investigating ligand interactions with TIR1 helps assess whether these compounds exhibit auxin-like activity and BRI1 (Brassinosteroid Receptor, PDB: 4OH4), which is essential for brassinosteroid-mediated cell expansion, vascular differentiation, and stress adaptation (5). Docking interactions with BRI1 provide insights into whether ganoderic acid A or progesterone can influence brassinosteroid signaling, thereby enhancing plant growth.

**2.7.1. Ligand preparation.** The structures of ganoderic acid A and progesterone were retrieved from the PubChem database in SDF format. The 3D structure was prepared for docking as a ligand using Chem3D 17.0, including energy minimization with the MMFF94 force field.

**2.7.2. Protein preparation.** The structures of the GID1 (Gibberellin Receptor, PDB: 3ED1), TIR1 (Auxin Receptor, PDB: 2P1Q), and BRI1 (Brassinosteroid Receptor, PDB: 4OH4) proteins were retrieved from the RCSB Protein Data Bank. The proteins were prepared for docking using AutoDock Tools 1.5.7 (4), which involved removing water molecules, adding polar hydrogens, and assigning a Kollman charge.

**2.7.3. Molecular docking.** Molecular docking studies were performed using PyRx 0.8 (6), a virtual screening tool that integrates AutoDock and AutoDock Vina for predicting protein-ligand interactions. A blind docking approach was utilized to identify potential binding sites across the entire surface of the

target protein. The docking grid was configured to encompass the entire protein structure, with grid box dimensions automatically calculated by PyRx to ensure comprehensive coverage. Docking simulations were executed using the AutoDock Vina algorithm, which employs a stochastic search method to predict optimal ligand binding poses. The exhaustiveness parameter was set to 8.

**2.7.4. Visualization and analysis.** The docked complexes were visualized and analyzed using BIOVIA Discovery Studio Visualizer (v24.01.23298) (7). Binding affinities ( $\Delta G$  values) were assessed, and key intermolecular interactions, such as hydrogen bonds and hydrophobic interactions, were identified and reported to provide insights into ligand–protein binding.

## 2.8. Effect of formed composites on plant growth, seed germination, and shoot-root elongation

**2.8.1. Experimental design.** The experiment was designed to evaluate the effects of progesterone adsorbed on dried reishi mushroom powder and calcinated reishi mushroom on plant growth, seed germination, and shoot-to-root elongation of Egyptian clover (*Trifolium alexandrinum*). The experimental site was located in El Wadi El Gedid Governorate, New Valley, Egypt, specifically in Paris town, Fig. 1. Egyptian clover was selected due to its fast-growing nature and adaptability to the region's environmental conditions.<sup>26</sup> The experimental plot size was one karat.

**2.8.2. Soil and water preparation.** Virgin sandy soil was used, which had not been cultivated or fertilized previously. Soil and water samples were collected and analyzed at the Soil and Water Laboratory of the Regional Agricultural Research Station of New Valley, Ministry of Agriculture, Egypt. The soil and water were deemed suitable for all crops based on the laboratory analysis.

**2.8.3. Soil preparation and fertilization.** The soil was plowed and leveled using agricultural tractors, and a sprinkler irrigation system was installed. The fertilizers applied included 885.7 kg ha<sup>-1</sup> of single superphosphate, 240.0 kg ha<sup>-1</sup> of potassium sulfate, 128.1 kg ha<sup>-1</sup> of urea (nitrogen), and 4800.0 kg ha<sup>-1</sup> of calcium sulfate.



Fig. 1 Experimental site in Paris town, El Wadi El Gedid, Egypt, used for Egyptian clover cultivation.



Table 1 The applied treatments to Egyptian clover rows in the experimental setup

| Treatment   | Description  | Row number |
|---|--|------------|
| Control   | Row with no treatment                              | 1          |
| Dried reishi mushroom powder + progesterone (composite 1)               | Dried mushroom powder mixed with progesterone      | 2          |
| Dried reishi mushroom powder (only)                                     | Dried mushroom powder without progesterone         | 3          |
| Calcinated reishi mushroom powder (carbon) + progesterone (composite 2) | Calcinated mushroom powder mixed with progesterone | 4          |
| Calcinated reishi mushroom powder (carbon only)                         | Calcinated mushroom powder without progesterone    | 5          |

**2.8.4. Experimental setup.** A single variety of Egyptian clover seeds with uniform vigor was selected, mixed, and planted in rows. The seeds were inoculated with *Rhizobium* bacteria to enhance nitrogen fixation. Five rows were prepared for the experiment, each representing a different treatment, and color indicators were used to mark the rows. The treatments were set as mentioned in Table 1.

**2.8.5. Planting and data collection timeline.** The experiment consisted of five rows, each representing a distinct treatment. The planting took place on 1st September 2024 at El Wadi El Gedid, Egypt, using sandy loam soil. A regular irrigation schedule was followed, with watering every three days. Data collection focused on several key parameters, including seed germination percentage, shoot-to-root elongation (with shoot and root lengths measured weekly), and plant growth assessments such as plant height, number of leaves, fresh weight, and dry weight. Soil analysis was conducted both before and after the experiment to evaluate changes in soil pH, organic matter, nitrogen, phosphorus, and potassium levels, as shown in Table 2. Harvest quality was assessed by measuring the protein content, fiber content, and overall biomass yield for each treatment.

## 2.9. Assessment of the greenness profile of the method

The environmental friendliness of an analytical methodology is influenced by several characteristics, including the number and toxicity of chemicals used, the amount of waste produced, the amount of power consumed, the number of steps in the

process, miniaturization, and automation. Using the NEMI, AGP, and modified GAPI (Mo GAPI) approaches, an extensive study is conducted to quantitatively assess the overall sustainability level and greenness profile of our suggested method.<sup>18</sup> The Analytical Eco-scale and the Analytical GREENness Calculator (AGREE) were the two green measures utilized. The first approach presented is the eco-scale score.<sup>27</sup> The total number of penalty points was deducted from 100, with deductions for waste, toxicity, reagents, and power. The researcher can determine whether the method is optimal for becoming green. AGREE is yet another measure. A “green tool” is a rapid quantitative approach that returns a score indicating how well a method adheres to the 12 basic principles of green analytical chemistry.<sup>28</sup> The newly created BAGI evaluates the “blueness,” or applicability and practicality, of an analytical technique.<sup>29</sup> The BAGI tool can be used to quantitatively assess blueness based on ten helpful criteria, including evaluation type, total number of analytes, equipment demands, sample efficiency, prepared sample needs, analysis percentage, reagents/materials used, preliminary concentration needs, automation perspective, and sample volume.

## 3. Results and discussion

### 3.1. Characterization of prepared materials

The findings of the characterization of raw reishi mushroom (RM) and its calcinated form (ARM) are presented in Fig. 2. A powdered X-ray diffractogram was conducted for both RM and

Table 2 The data collection timeline

| Stage                    | Date         | Activities  | Data to collect   |
|--------------------------|--------------|---|---|
| Preparation              | 25/08/2024   | Prepare soil, treatments, and planting area         | Soil pH, organic matter, nitrogen, phosphorus, and potassium                        |
| Planting                 | 01/09/2024   | Plant clover seeds in rows with assigned treatments | Record planting date and initial conditions   |
| Weekly growth monitoring | Every 7 days | Measure plant growth and observe changes            | Plant height, number of leaves, fresh weight, dry weight, and notes on plant health |
| Soil analysis            | 01/09/2024   | Analyze the soil before planting                    | Soil pH, organic matter, nitrogen, phosphorus, and potassium                        |
| Soil analysis            | 15/10/2024   | Analyze soil after harvest                          | Soil pH, organic matter, nitrogen, phosphorus, and potassium                        |
| Harvest                  | 15/10/2024   | Harvest clover after 45 days                        | Fresh weight, dry weight, protein content, and fiber content                        |



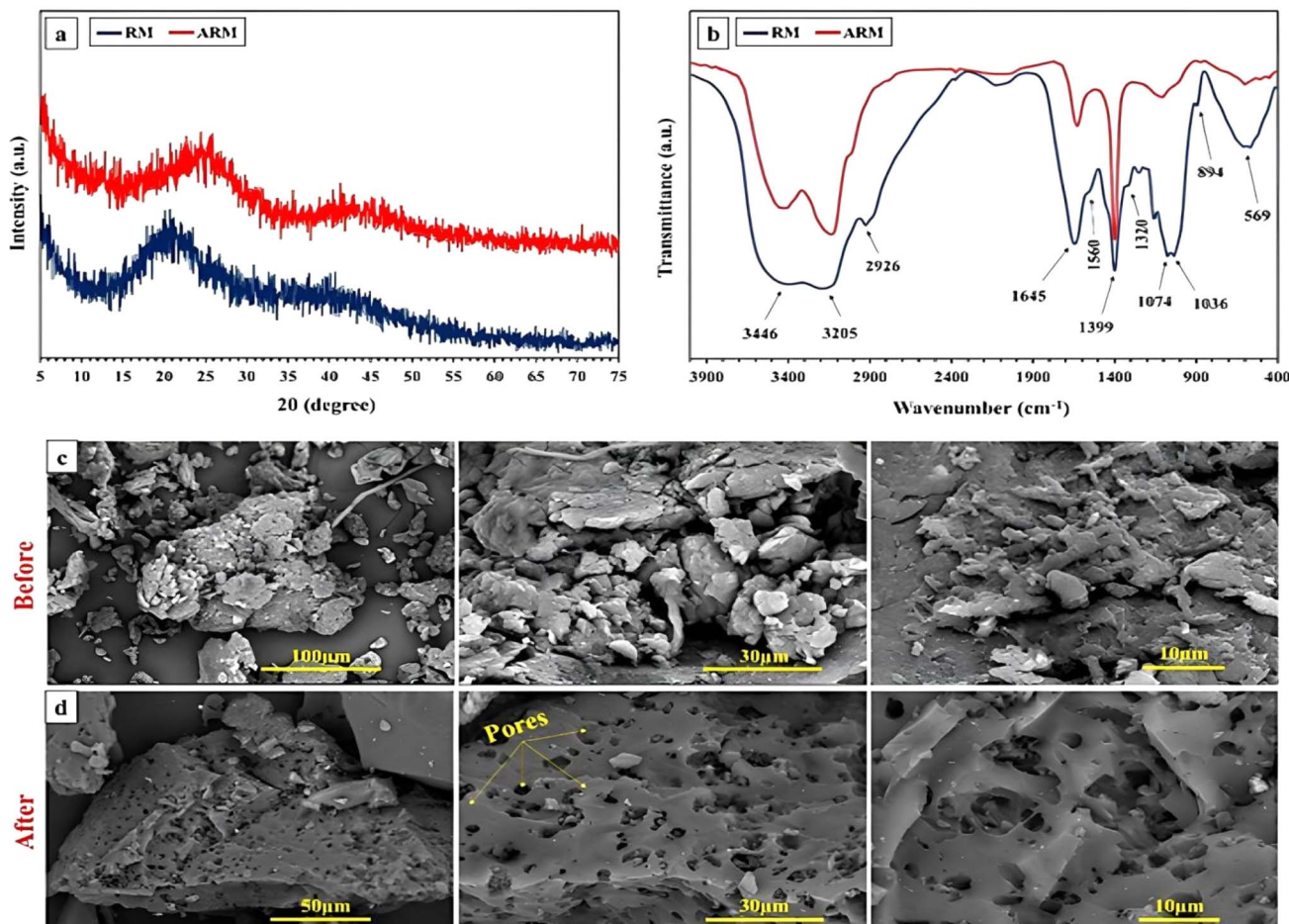


Fig. 2 The physicochemical characteristics of raw reishi mushroom (RM) and its calcinated form (ARM). (a) XRD, (b) FTIR, and (c and d) SEM images.

ARM in the  $2\theta$  range of  $5^\circ$  to  $75^\circ$  to evaluate the crystalline nature of the materials. The XRD patterns (Fig. 2a) indicate the amorphous nature of both materials, as a significant portion of the composition consists of a carbon substrate. The XRD pattern of RM exhibits a broad peak at approximately  $2\theta = 20.74^\circ$ , associated with its carbon structure, with no additional peaks observed at higher scattering angles. Meanwhile, the XRD pattern of ARM reveals two distinct diffraction peaks at  $2\theta = 24.01^\circ$  and  $2\theta = 42.71^\circ$ , which correspond to the (002) and (100) crystal planes of graphite.<sup>30</sup> A graphitized crystal structure is indicated by the (100) microcrystalline plane of graphite, whereas the (002) microcrystalline plane of graphite implies the presence of disordered microcrystalline carbon.<sup>31</sup> These results suggest that the thermal carbonization method produced semi-graphitized microcrystalline structures and a significant quantity of amorphous carbon.

FTIR techniques were widely employed to characterize the functional groups of the compounds RM and ARM. Fig. 2b presents the FTIR spectrum data in the wavenumber range of  $400\text{--}4000\text{ cm}^{-1}$ . The spectrum of raw RM reveals a broad band between  $3600$  and  $3200\text{ cm}^{-1}$ , corresponding to the vibrational stretching of hydroxyl groups ( $-\text{OH}$ ).<sup>32</sup> Additionally, peaks at  $2926\text{ cm}^{-1}$  and  $1399\text{ cm}^{-1}$  are attributed to the stretching and

bending vibrations of saturated C–H bonds, respectively.<sup>30</sup> The band at  $1645\text{ cm}^{-1}$  corresponds to the amide I stretching of C=O, while the band at  $1560\text{ cm}^{-1}$  is associated with the stretching or N–H deformation of amide II. The vibration of the C–N bond is represented by the amide III band at  $1315\text{ cm}^{-1}$ .<sup>30,33</sup> Furthermore, the vibrations of the C–O bond in alcohol hydroxyl appear at  $1036\text{ cm}^{-1}$  and  $1074\text{ cm}^{-1}$ . The absorption peak at  $894\text{ cm}^{-1}$  is characteristic of the  $\beta$ -configuration of D-glucose units, indicating a significant presence of glucan structure.<sup>30,34</sup> According to Fathi *et al.*,<sup>35</sup> the  $893\text{ cm}^{-1}$  band in the fingerprint region of D-glucopyranose is one of the most significant recorded bands. Lastly, the band at  $569\text{ cm}^{-1}$  represents the bending vibration of a saccharide group.<sup>34</sup> The FT-IR spectrum of ARM exhibits peaks at  $3417\text{ cm}^{-1}$  and  $3132\text{ cm}^{-1}$ , which correspond to the stretching vibrations of the  $-\text{OH}$  group. Additionally, a peak at  $1631\text{ cm}^{-1}$  is associated with the stretching of the C=O group, while the peak at  $1399\text{ cm}^{-1}$  corresponds to C–H bonds. In comparison to the spectrum of RM, the characteristic peaks of ARM are notably weaker, and some peaks have disappeared entirely. This observation indicates that the reishi mushroom sample has transformed into carbon material as a result of the chemical pyrolysis process.

Fig. 2(c and d) depicts the microstructures of raw RM (c) and ARM (d) as observed at various magnifications using a scanning electron microscope. The microstructure of RM reveals that the mycelial fibers are haphazardly wrapped, forming a multi-layer pore structure and a developed network that is ideal for the creation of porous materials. Following the chemical pyrolysis process, ARM displays a markedly increased porous structure, demonstrating that reishi mushrooms are an efficient source of carbon for the production of porous materials, particularly activated carbon. The porous surface morphology of the produced carbon is advantageous for progesterone adsorption, as the micro and mesopores of its calcinated form serve as effective adsorption sites.

Progesterone hormone (HP) adsorption was assessed for both materials (RM and ARM). The FTIR analysis findings (Fig. 3a and b) and the microstructure following progesterone hormone adsorption are displayed in Fig. 3c and d. As shown in Fig. 3a, after the adsorption of progesterone (HP) onto raw reishi mushroom (RM), the intensity of major peaks increases, and new peaks appear, indicating an interaction between RM and HP. Peaks in the range of  $2928\text{--}2853\text{ cm}^{-1}$  correspond to the stretching of the C–H bonds in the  $\text{CH}_2$  and  $\text{CH}_3$  groups.

Additionally, peaks at  $1698\text{ cm}^{-1}$  and  $1661\text{ cm}^{-1}$  are observed, which are associated with the stretching of the  $\text{C}=\text{O}$  bond. Furthermore, a peak at  $1612\text{ cm}^{-1}$  is noted, corresponding to the stretching of the  $\text{C}=\text{C}$  bond. Similarly, Fig. 3b demonstrates an increase in peak intensity as a result of HP adsorption. The scanning electron microscope (SEM) images of RM after adsorption reveal a network complexation between the mycelial fibers in RM and the HP particles (Fig. 3c). Conversely, the pores of calcinated reishi mushroom produced from RM (ARM) are filled with HP particles, as illustrated in the SEM images (Fig. 3d) of ARM following adsorption.

### 3.2. Adsorption study

**3.2.1. The effect of pH on the adsorption.** The effect of pH on the adsorption processes of progesterone on each reishi mushroom and its calcined form was investigated over a pH range of 3–9, Fig. 4(c and d). The results demonstrated that, at pH 3, which is below the point of zero charge ( $\text{pH}_{\text{pzc}}$ ) for both reishi mushroom ( $\text{pH}_{\text{pzc}} = 5$ ) and its calcined form ( $\text{pH}_{\text{pzc}} = 7$ ), the surfaces of both adsorbents will be positively charged as shown in Fig. 4(a and b) respectively. Although the progesterone molecule is protonated at this pH and the adsorbent surfaces

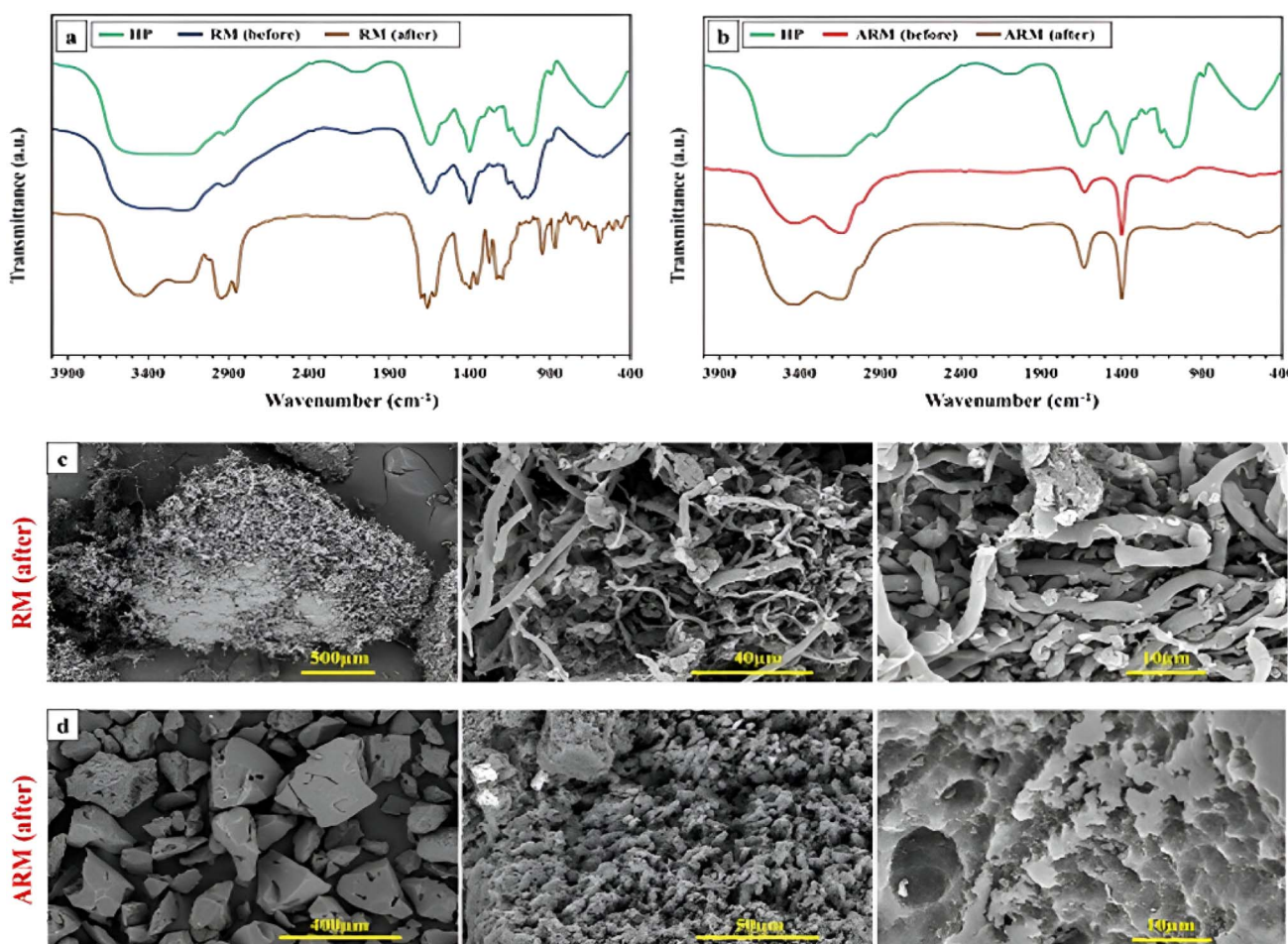


Fig. 3 FTIR spectrum (a and b) and SEM images of raw reishi mushroom (RM) and its calcinated form (ARM) after progesterone hormone adsorption (HP).



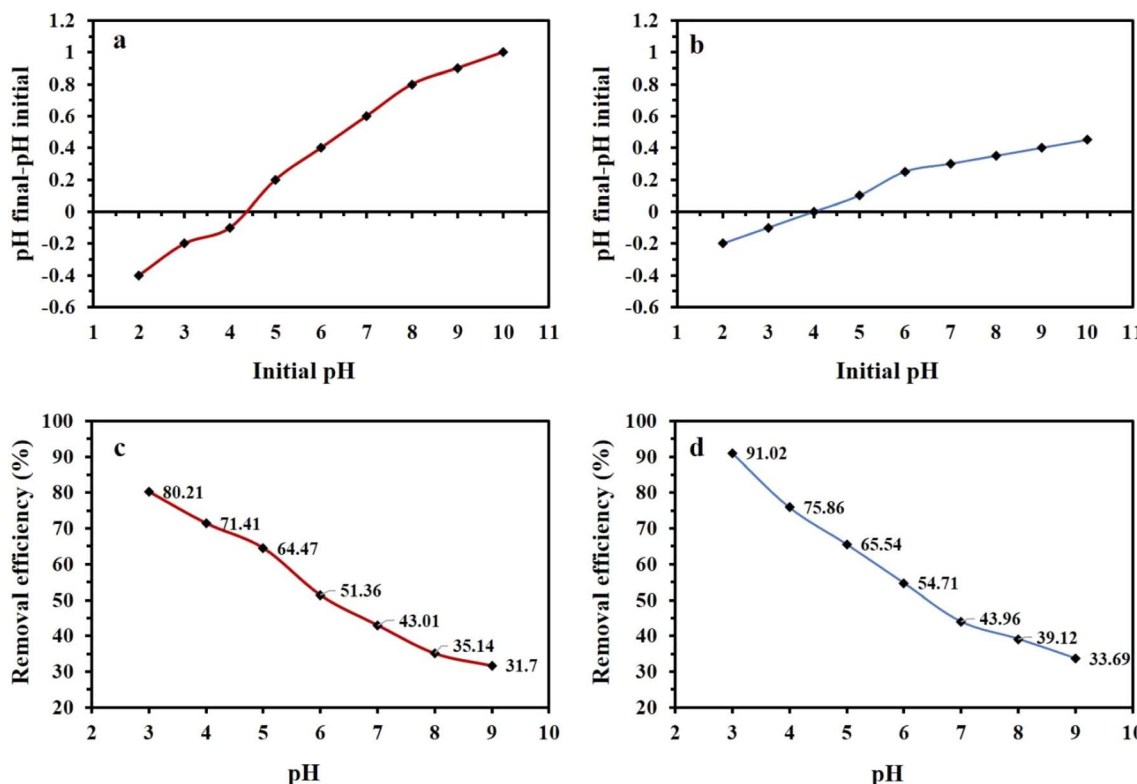


Fig. 4 (a) shows the PZC of reishi mushroom, (b) shows the PZC of calcinated reishi mushroom (c) shows the removal efficiency of progesterone ( $100 \mu\text{g mL}^{-1}$ ) by ( $0.05 \text{ g}/50 \text{ mL}$ ) of reishi mushroom at different pH of the solution, (d) shows the removal efficiency of progesterone ( $100 \mu\text{g mL}^{-1}$ ) by ( $0.05 \text{ g}/50 \text{ mL}$ ) of calcinated reishi mushroom at different pH of the solution.

are positively charged, leading to potential electrostatic repulsion, the highest adsorption efficiency was observed. This suggests that non-electrostatic interactions, particularly van der Waals forces and hydrophobic interactions, play a dominant role in the adsorption process. At this pH, van der Waals forces and hydrophobic interactions between the adsorbent surface and progesterone molecules compensate for the potential electrostatic repulsion, thereby improving adsorption efficiency. As the pH increases to 5 and 6, approaching the pH<sub>pzc</sub> of both materials, the surface charge of the adsorbents will become less positive and move toward neutrality, which will reduce the electrostatic attraction between the adsorbent and progesterone. While the adsorption is still possible due to hydrophobic interactions, the efficiency begins to decrease. At pH 7, the surfaces of both adsorbents will be more neutral or slightly negative, further reducing the adsorption efficiency, as the neutral progesterone will have weaker interactions with the adsorbent surface. At pH 9, both adsorbents will have a negative charge, which could result in significant electrostatic repulsion between the negatively charged adsorbent surface and the neutral progesterone molecule, leading to a sharp reduction in adsorption efficiency. Therefore, pH 3 is considered the optimum pH for the adsorption of progesterone on both reishi mushroom and calcinated reishi mushroom, where van der Waals forces and hydrophobic interactions are the predominant mechanisms enhancing progesterone removal most effectively.

**3.2.2. Effect of dose of adsorbent on the adsorption processes.** The experimental results have demonstrated the maximum adsorption efficiencies with adsorbent doses of 0.1 g for reishi mushroom and 0.075 g for its calcined form at pH 3, maintaining cost-effectiveness and ensuring a balance between the adsorbent surface area and the amount of progesterone to be removed. The dose range of 0.05 g to 0.30 g was investigated to determine the impact of adsorbent quantity on progesterone removal as shown in Fig. 5a and b. At lower doses (0.05 g), the available surface area for adsorption is limited, leading to lower removal efficiency. As the dose increases, there is more surface area available for interaction with progesterone, thus improving removal efficiency. However, increasing the dose to 0.30 g leads to diminishing returns, where excess adsorbent does not significantly enhance adsorption because the active sites on the adsorbent are saturated or the concentration of progesterone becomes a limiting factor. The 0.1 g dose for reishi mushroom and 0.075 g for calcinated reishi mushroom were chosen as optimal values, which avoid the overuse of adsorbent that could lead to unnecessary costs and material waste.

**3.2.3. Thermodynamics of the adsorption process.** The experimental results revealed that the maximum removal efficiency of progesterone for both adsorbents was obtained at a temperature of 25 °C with doses of 0.1 g for reishi mushroom and 0.075 g for calcinated reishi mushroom at pH 3, which ensures that the process remains energy-efficient and consistent with typical environmental conditions. The effect of



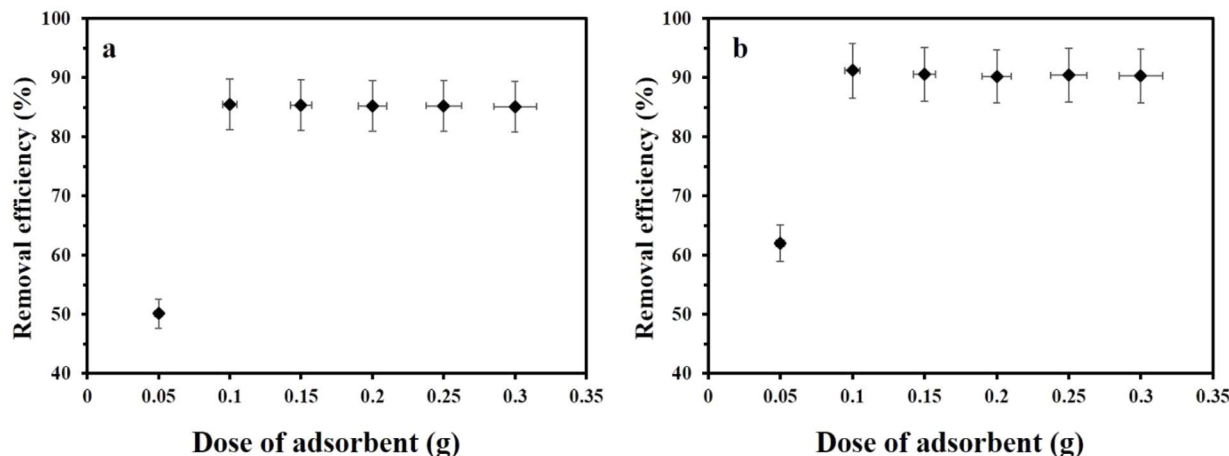


Fig. 5 The effect of dose of adsorbents on the removal efficiency of progesterone using (a) reishi mushroom (b) calcinated reishi mushroom.

temperature on the removal efficiency of progesterone was investigated over a range from 25 °C to 55 °C, as shown in Fig. 6a and b. At 25 °C (low temperature), the adsorption process favors stable interactions between the adsorbents and progesterone molecules.<sup>36,37</sup> Considering that progesterone becomes protonated under acidic conditions, the adsorption mechanism is mainly governed by van der Waals forces, electrostatic interactions, and hydrophobic forces. As the temperature increases, the kinetic energy of the molecules rises, leading to the disruption of these intermolecular forces and resulting in reduced adsorption efficiency due to enhanced desorption and weakening of binding forces.<sup>38</sup> Additionally, higher temperatures may lead to excessive thermal motion, degradation of the adsorbent surface, or loss of active sites, further contributing to the observed decline in adsorption performance.<sup>39</sup>

The equilibrium constant,  $K_d = (q_e/c_e)$ , was calculated at various temperatures using the van't Hoff equation, which helped in identifying the underlying adsorption mechanism:

$$\ln K_d = \Delta S^\circ/R - \Delta H^\circ/RT \quad (3)$$

where:  $K_d$ : the equilibrium constant ( $\text{L mg}^{-1}$ ),  $R$ : is the gas rate constant ( $8.314 \text{ J mol}^{-1} \text{ K}^{-1}$ ),  $\Delta H^\circ$ : the enthalpy changes of adsorption ( $\text{kJ mol}^{-1}$ ),  $\Delta S^\circ$ : the entropy of adsorption, and Gibbs free energy ( $\Delta G^\circ$ ) could be obtained using eqn (4).

$$\Delta G^\circ = -RT \ln K_d = \Delta H^\circ - T\Delta S^\circ \quad (4)$$

$$\ln K_d = -\Delta H^\circ/R(1/T) + \Delta S^\circ/R \quad (5)$$

The calculated thermodynamic parameters are summarized in Table 3. The negative values of  $\Delta G^\circ$  at lower temperatures indicate that the adsorption of progesterone onto both reishi mushroom and calcinated reishi mushroom is spontaneous. However, as the temperature increases,  $\Delta G^\circ$  becomes less negative or even positive, suggesting a decrease in spontaneity at elevated temperatures. The negative  $\Delta H^\circ$  values confirm that the adsorption process is exothermic, meaning that heat is released during adsorption, favoring the process at lower temperatures. Furthermore, the negative  $\Delta S^\circ$  values suggest a decrease in randomness at the solid–solution interface during the adsorption process, indicating that the progesterone

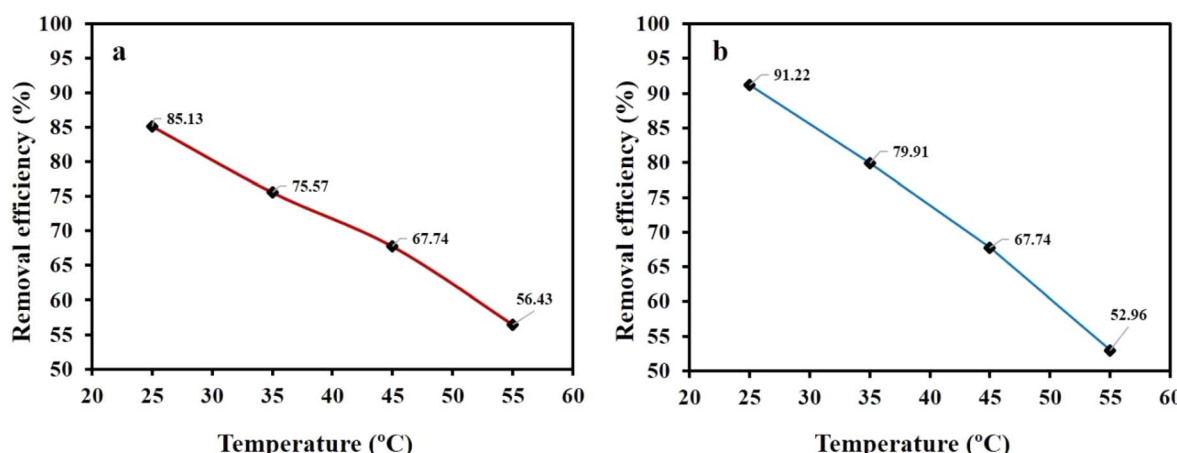


Fig. 6 Effect of temperature on the adsorption process of progesterone using (a) reishi mushroom (b) calcinated reishi mushroom.



**Table 3** The thermodynamic parameters for the adsorption process of progesterone using reishi mushroom and calcinated reishi mushroom as adsorbents

| Contaminant  | T (K) | $\Delta G^\circ$ (kJ mol <sup>-1</sup> ) |                            | $\Delta H^\circ$ (kJ mol <sup>-1</sup> ) |                            | $\Delta S^\circ$ (kJ mol <sup>-1</sup> K <sup>-1</sup> ) |                            |
|--------------|-------|--|----------------------------|--|----------------------------|--|----------------------------|
|              |       | Reishi mushroom                          | Calcinated reishi mushroom | Reishi mushroom                          | Calcinated reishi mushroom | Reishi mushroom  | Calcinated reishi mushroom |
| Progesterone | 298   | -2523.18                                 | -3899.17                   | -39421.66                                | -59505.8                   | -123.82  | -186.599                   |
|              | 308   | -1284.98                                 | -2033.17                   |  |                            |  |                            |
|              | 318   | -46.77                                   | -167.17                    |  |                            |  |                            |
|              | 328   | 1191.42                                  | 1698.81                    |  |                            |  |                            |

molecules are well-ordered on the surface of the adsorbent.<sup>40-42</sup> These findings are consistent with previous reports where the adsorption of organic molecules onto natural or bio-derived adsorbents was governed by similar exothermic and spontaneous behavior with reduced entropy changes.<sup>43,44</sup>

**3.2.4. Effect of contact time.** The effect of contact time on the adsorption of progesterone using reishi mushroom and calcinated reishi mushroom was investigated over a range of 0–240 minutes using different models, including pseudo first order and second order, mixed order, Avrami model, and intraparticle diffusion, as shown in Table 4. The results revealed that the adsorption process for both adsorbents initially exhibited a rapid increase in removal efficiency due to the availability of abundant active sites on the adsorbent surface. For reishi mushroom, the removal efficiency increased steadily, reaching approximately 80.12% at 180 minutes and stabilizing at 82.68% at 240 minutes, indicating that equilibrium was achieved at around 200 minutes. In contrast, the calcinated reishi mushroom demonstrated faster adsorption kinetics, with removal efficiency reaching 87.34% at 120 minutes and plateauing at 88.09% thereafter, suggesting that equilibrium was attained earlier, as shown in Fig. S1a and b.<sup>†</sup> This faster adsorption is attributed to the enhanced surface area and pore structure of the calcinated reishi mushroom, which facilitates quicker interaction with progesterone molecules. The

adsorption kinetics likely follow pseudo-second-order and mixed-order models, highlighting the dominance of chemisorption and possible diffusion effects.<sup>45-47</sup> The effect of contact time is shown in Fig. 7 as the dependence of the removal efficiency on the contact time (*t*).

**3.2.5. Adsorption isotherm.** The adsorption capacities of the adsorbents were investigated using the non-linear adsorption isotherm models.<sup>25</sup> Nine non-linear equilibrium isotherm models were utilized to fit the experimental data for each adsorbent. Three of them used the (two-parameter) isotherm models as Langmuir,<sup>26</sup> Freundlich and Dubinin–Radushkevich, four used the (three-parameter) isotherm models as Langmuir–Freundlich and Sips,<sup>27</sup> Redlich–Peterson,<sup>28</sup> Toth;<sup>29</sup> only one used the four parameters isotherm Baudu<sup>30</sup> and one used the five parameters isotherm Fritz–Schlunder. It was demonstrated that both the Langmuir model and the Freundlich isotherm models are the most adequate adsorption isotherm models for progesterone onto the investigated adsorbents showing the highest adsorption capacity with higher *R*<sup>2</sup> values~ 0.99, as shown in Fig. S2.<sup>†</sup> Moreover, the experimental data of the adsorption isotherms have confirmed the significant efficacy of the adsorbents in the removal of progesterone, with high adsorption capacities *q*<sub>max</sub> of 90.52, 118.10 mg g<sup>-1</sup> for progesterone using reishi mushroom and calcinated reishi mushroom respectively at pH 3, 0.1 g of reishi mushroom and 0.075 g of

**Table 4** The kinetic models' parameters

| Kinetic models          | Equation   | Parameters | Reishi mushroom | Calcinated reishi mushroom |
|-------------------------|--|------------|-----------------|----------------------------|
| Pseudo first order      | $q_t = q_e(1 - e^{-k_1 t})$                                | $K_1$      | 0.44            | 0.048                      |
|                         |  | $Q_e$      | 52.06           | 98.02                      |
|                         |  | $R^2$      | 0.98            | 0.98                       |
| Pseudo second order     | $q_t = \frac{q_e^2 k_2 t}{1 + q_e k_2 t}$                  | $K_2$      | 0.007           | 0.004                      |
|                         |  | $Q_e$      | 59.24           | 105.16                     |
|                         |  | $R^2$      | 0.99            | 0.99                       |
| Mixed 1, 2 order        | $q_t = \frac{q_e(1 - \exp(-k_1 t))}{1 - f_2 \exp(-k_1 t)}$ | $K$        | 0.041           | 0.049                      |
|                         |  | $Q_e$      | 54.23           | 98.02                      |
|                         |  | $F_2$      | 0.0001          | 0.0001                     |
| Avrami                  | $q_t = q_e[1 - \exp(-k_{av} t)^{n_{av}}]$                  | $R^2$      | 0.99            | 0.99                       |
|                         |  | $Q_e$      | 51.80           | 97.29                      |
|                         |  | $K_{av}$   | 0.209           | 0.45                       |
| Intraparticle diffusion | $q_t = K_{ip} \sqrt{t} + C_{ip}$                           | $n_{av}$   | 0.198           | 0.107                      |
|                         |  | $R^2$      | 0.98            | 0.98                       |
|                         |  | $K_{ip}$   | 2.86            | 4.76                       |
|                         |  | $C_{ip}$   | 16.22           | 39.22                      |
|                         |  | $R^2$      | 0.65            | 0.68                       |



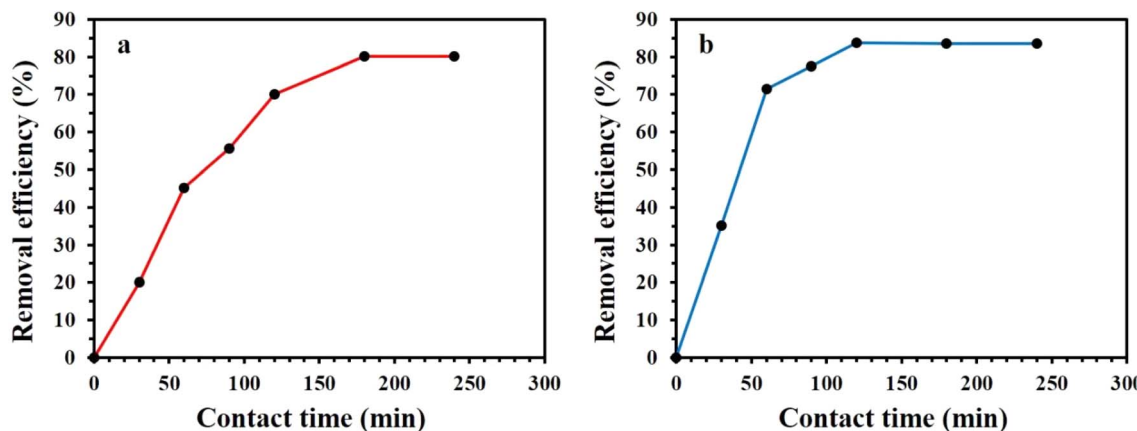


Fig. 7 Effect of contact time on the removal of progesterone using (a) reishi mushroom (b) reishi mushroom-derived activated carbon.

calcinated reishi mushroom at 25 °C (as optimum conditions for adsorption) as shown in Table 5.

### 3.3. Molecular docking study

Molecular docking analysis revealed the binding affinities ( $\text{kcal mol}^{-1}$ ) of ganoderic acid A and progesterone with three key plant receptors: GID1, TIR1, and BRI1. The binding affinities are summarized in Table 6. The docking simulations identified favorable binding interactions for both ligands, with progesterone consistently showing slightly stronger binding affinities compared to ganoderic acid A. The detailed interaction profiles of each ligand-receptor complex is presented in Fig. 1–6, highlighting key stabilizing interactions.

**3.3.1. GID1 receptor interactions.** Ganoderic acid A (Fig. S3†) forms hydrogen bonds with Asn-349, Ser-345, and Glu-342, contributing to strong stabilization within the GID1 receptor. The unfavorable donor–donor interaction with Val-335 is unlikely to hinder binding, suggesting that Ganoderic Acid A may modulate gibberellin signaling. Progesterone (Fig. S4†) interacts with GID1 through conventional hydrogen bonds involving Ser-198, Tyr-329, and Arg-35, along with a carbon–hydrogen bond with Lys-28, providing significant stability. These findings suggest its potential role as a bioactive compound in plant growth regulation.

**3.3.2. TIR1 receptor interactions.** Ganoderic acid A (Fig. S5†) exhibits strong binding to TIR1 through hydrogen bonds with Arg-9, Arg-403, and Arg-164, which are key residues in auxin signaling. These interactions indicate that ganoderic acid A may influence plant growth and elongation. Progesterone (Fig. S6†) binds to TIR1 through hydrogen bonds with Arg-344 and Arg-403. Additionally, Pi–sigma and Pi–alkyl interactions involving Phe-346, Arg-9, and Val-8 enhance the binding stability. These interactions reinforce the idea that Progesterone could modulate auxin receptor activity and contribute to plant growth regulation.

**3.3.3. BRI1 receptor interactions.** Ganoderic acid A (Fig. S7†) forms stabilizing hydrogen bonds with Ser-1013, Ser-1026, and Met-959, as well as a carbon–hydrogen bond with Ser-1013. These interactions enhance its stability within the BRI1

binding pocket. Progesterone (Fig. S8†) shows strong conventional hydrogen bonds with Lys-1011 and Met-959, along with an alkyl interaction with Val-897, reinforcing the ligand's stability. While there is a minor acceptor–acceptor interaction with Asn-1014, the overall interaction profile supports a well-stabilized complex.

**3.3.4. Potential role of ganoderic acid a and progesterone as plant growth enhancers: molecular docking insights.** Through molecular docking analysis, the binding affinities of ganoderic acid A (a major bioactive compound in *Ganoderma lucidum*) and progesterone were assessed against GID1 (gibberellin receptor), TIR1 (auxin receptor), and BRI1 (brassinosteroid receptor) to explore their potential role as plant growth enhancers. The docking results demonstrated that progesterone exhibited the highest binding affinity to GID1 ( $-10.4 \text{ kcal mol}^{-1}$ ), suggesting a strong potential for modulating gibberellin signaling, which is crucial for seed germination and stem elongation. Additionally, both ganoderic acid A ( $-8.5 \text{ kcal mol}^{-1}$ ) and progesterone ( $-8.6 \text{ kcal mol}^{-1}$ ) bound effectively to TIR1, indicating possible interactions with the auxin signaling pathway, which regulates cell division and elongation. Similarly, docking with BRI1 showed competitive binding affinities for both compounds ( $-8.6 \text{ kcal mol}^{-1}$  for ganoderic acid A and  $-8.7 \text{ kcal mol}^{-1}$  for Progesterone), suggesting a possible role in brassinosteroid-mediated plant growth enhancement.

The results provide preliminary computational evidence that both reishi mushroom-derived compounds and progesterone can interact with key plant hormone receptors, potentially influencing plant growth and development. The strong binding affinity of progesterone to GID1 suggests that it may play a role in gibberellin-like activity, while ganoderic acid A's interactions with TIR1 and BRI1 highlight its potential influence on auxin and brassinosteroid signaling pathways.

### 3.4. Soil and water analyses results

**3.4.1. Soil analysis results.** The initial soil analysis of the experimental field revealed key characteristics that are critical for understanding the baseline conditions of the study (Table



Table 5 The non-linear adsorption isotherm models for progesterone using reishi mushroom and calcinated reishi mushroom

| Isotherm models                  | Expression   | Adjustable model parameters                         | Reishi mushroom                                   | Calcinated reishi mushroom                      |
|----------------------------------|--|---|---|---|
| <b>Two-parameters isotherm</b>   |  |   |   |   |
| Langmuir                         | $q_e = q_{\max} \frac{K_L C_e}{1 + K_L C_e}$                       | $q_{\max}$<br>$K_L$<br>$R^2$                        | 90.52<br>0.0017<br>0.99                           | 118.10<br>0.0077<br>0.99                        |
| Freundlich                       | $q_e = K_f C_e^{1/n_f}$  | $K_f$<br>$1/n_f$<br>$R^2$                           | 0.33<br>0.79<br>0.99                              | 2.329<br>0.656<br>0.99                          |
| Dubinin–Radushkevich (D–R)       | $q_e = q_{\max} \exp(-K_{DR} \varepsilon^2)$                       | $q_{\max}$<br>$K_{ad}$<br>$R^2$                     | 56.77<br>0.020<br>0.98                            | 85.80<br>0.009<br>0.99                          |
| <b>Three-parameters isotherm</b> |  |   |   |   |
| Langmuir–Freundlich              | $q_e = \frac{q_{\max} (K_{LF} C_e)^{MLF}}{1 + (K_{LF} C_e)^{MLF}}$ | $q_{\max}$<br>$K_{LF}$<br>$\beta_{LF}$<br>$R^2$     | 62.58<br>0.0032<br>1.15<br>0.99                   | 74.37<br>0.017<br>1.90<br>0.99                  |
| Sips                             | $q_e = \frac{q_{\max} K_s (C_e)^{1/n_s}}{1 + K_s (C_e)^{1/n_s}}$   | $q_{\max}$<br>$K_s$<br>$n_s$<br>$R^2$               | 62.59<br>0.0013<br>1.15<br>0.99                   | 74.41<br>0.0004<br>1.90<br>0.99                 |
| Redlich–Peterson                 | $q_e = \frac{K_R C_e}{1 + a_R C_e^{\beta_R}}$                      | $K_R$<br>$a_R$<br>$\beta_R$<br>$R^2$                | 0.144<br>0.00005<br>1.53<br>0.99                  | 0.669<br>0.00007<br>2.21<br>0.99                |
| Toth                             | $q_e = \frac{K_T C_e}{(a_T + C_e^Z)^{1/Z}}$                        | $K_e$<br>$K_t$<br>$n_t$<br>$R^2$                    | 0.219<br>0.00007<br>1.51<br>0.99                  | 0.290<br>0.00008<br>1.39<br>0.98                |
| <b>Four-parameters isotherm</b>  |  |   |   |   |
| Baudu                            | $q_e = \frac{q_{\max} b_o C_e^{1+x+y}}{1 + b_o C_e^{1+x}}$         | $q_{\max}$<br>$b_o$<br>$X$<br>$Y$<br>$R^2$          | 62.57<br>0.0013<br>0.0001<br>0.152<br>0.99        | 74.4<br>0.0004<br>0.0001<br>0.90<br>0.99        |
| <b>Five-parameters isotherm</b>  |  |   |   |   |
| Fritz–Schlunder (V)              | $q_e = \frac{q_{\max} K_1 C_e^{m1}}{1 + K_2 C_e^{m2}}$             | $q_{\max}$<br>$K_1$<br>$K_2$<br>$n$<br>$m$<br>$R^2$ | 6.28<br>0.099<br>0.876<br>0.797<br>0.0005<br>0.99 | 6.80<br>0.055<br>0.69<br>1.21<br>0.0006<br>0.99 |

Table 6 Binding affinities of ganoderic acid A and progesterone with GID1, TIR1, and BRI1 receptors

| Receptor | Ligand           | Binding affinity (kcal mol <sup>-1</sup> ) |
|----------|------------------|--|
| GID1     | Ganoderic acid A | -8.40                                      |
|          | Progesterone     | -10.40                                     |
| TIR1     | Ganoderic acid A | -8.50                                      |
|          | Progesterone     | -8.60                                      |
| BRI1     | Ganoderic acid A | -8.60                                      |
|          | Progesterone     | -8.70                                      |

S1†). The soil had a pH of 7.63, indicating a slightly alkaline nature, which is typical for arid and semi-arid regions. The electrical conductivity (ECe) of 1.44 dS m<sup>-1</sup> and salt

concentration of 226 ppm suggested low to moderate salinity, which is within acceptable limits for Egyptian clover cultivation. The cation exchange capacity (CEC) was dominated by sodium (Na) at 7.17 meq L<sup>-1</sup>, followed by calcium (Ca) at 5.16 meq L<sup>-1</sup> and magnesium (Mg) at 2.49 meq L<sup>-1</sup>. The anion composition was primarily chloride (Cl) at 5.57 meq L<sup>-1</sup> and sulfate (SO<sub>4</sub>) at 7.84 meq L<sup>-1</sup>. The soil also contained 3.12% calcium carbonate (CaCO<sub>3</sub>), which is consistent with the calcareous nature of soils in the region.

**3.4.2. Water analysis results.** The irrigation water analysis (Table S2†) showed a pH of 6.92, indicating a neutral to slightly acidic nature, which is suitable for crop irrigation. The electrical conductivity (EC) of 0.75 dS m<sup>-1</sup> and total dissolved solids (TDS) of 480 ppm confirmed the low salinity of the water. The cation



composition was dominated by calcium (Ca) at 3.13 meq L<sup>-1</sup> and sodium (Na) at 2.52 meq L<sup>-1</sup>, while the anion composition was primarily chloride (Cl) at 3.37 meq L<sup>-1</sup> and bicarbonate (HCO<sub>3</sub>) at 2.14 meq L<sup>-1</sup>. The sodium adsorption ratio (SAR) of 1.65 and residual sodium carbonate (RSC) of 0 indicated that the water posed no risk of sodicity or alkalinity hazards. The iron (Fe) concentration of 0.42 ppm was within acceptable limits for irrigation.

### 3.5. Growth performance and soil quality assessment

**3.5.1. Seed germination.** The composite 2 treatment (progesterone adsorbed on calcinated reishi mushroom) showed the highest seed germination rate (95%), followed by composite 1 (90%), and the control group (80%). Whereas the reishi mushroom powder only and calcinated reishi mushroom only treatments showed moderate germination rates of 85% and 88%, respectively.

**3.5.2. Shoot-to-root elongation.** Composite 2 resulted in the highest shoot-to-root elongation ratio (2.5 : 1), indicating enhanced nutrient uptake and growth stimulation. Composite 1 also showed a significant improvement in shoot-to-root elongation (2.2 : 1) compared to the control (1.8 : 1). The reishi mushroom powder only and calcinated reishi mushroom only treatments showed ratios of 2.0 : 1 and 2.1 : 1, respectively.

**3.5.3. Plant growth.** Composite 2 treatment resulted in the highest average plant height (39 cm), fresh weight (200 g), and dry weight (40 g). Composite 1 treatment showed an average plant height of 36 cm, fresh weight of 180 g, and dry weight of 35 g. The reishi mushroom powder only and its calcinated form only treatments showed moderate growth compared to the control, as shown in Table S3.†

**3.5.4. Soil quality.** The soil pH slightly decreased after harvest in treatments involving reishi mushroom powder, likely due to the release of organic acids during decomposition. Organic matter content increased significantly in treatments with reishi mushroom powder and its composites, indicating improved soil fertility.

**3.5.5. Harvest quality.** Composite 2 yielded the highest protein content (22%) and the lowest fiber content (9%). Composite 1 also showed improved protein content (20%) and reduced fiber content (10%) compared to the control (18% protein and 12% fiber), as shown in Table S4.†

**3.5.6. Statistical analysis of plant growth performance.** The statistical analysis of plant growth performance under different

treatments, including a summary of key growth parameters and their statistical significance, is presented in Table 7.

**3.5.7. Comparison with previous studies.** The results align with previous studies that highlight the benefits of fungal-based amendments in agriculture.<sup>48</sup> However, the use of progesterone in combination with reishi mushroom and calcinated reishi mushroom is a novel approach that demonstrates significant potential for improving crop productivity.

**3.5.8. Mechanism of action.** The improved growth and germination rates in treatments involving progesterone suggest that the hormone may enhance cell division and elongation, particularly in the root system, leading to better nutrient uptake and overall plant health. The calcinated reishi mushroom likely acted as a carrier for progesterone, ensuring its gradual release and prolonged effect on plant growth.<sup>11,49</sup>

**3.5.9. Effect of progesterone adsorption on plant growth.** The adsorption of progesterone on reishi mushroom powder and its calcinated form significantly enhanced plant growth, seed germination, and shoot-to-root elongation. This suggests that progesterone, when combined with reishi mushroom-based amendments, acts as a growth stimulant. The higher performance of composite 2 (progesterone adsorbed on calcinated reishi mushroom) can be attributed to the increased surface area and adsorption capacity of the calcinated reishi mushroom, which likely facilitated a more controlled release of progesterone.

**3.5.10. Role of reishi mushroom and its calcinated form in soil fertility.** The reishi mushroom powder and its calcinated form improved soil fertility by increasing organic matter content and enhancing nutrient availability.<sup>50</sup> The calcinated form of reishi mushroom showed superior performance, likely due to its porous structure, which improved water retention and nutrient adsorption in the soil. Organic matter content increased notably in treatments involving reishi mushroom powder and its calcinated form, contributing to better plant growth and overall soil health.

### 3.6. The greenness profile of the proposed method

Sustainability cannot be fully examined using a single evaluation tool across all pertinent aspects.<sup>51</sup> An analytical technique or procedure known as GAC reduces or eliminates solvents, chemicals, or other hazardous substances that are hazardous to the environment or public health. GAC maintains quality standards while remaining quick and affordable.<sup>52</sup> Analytical

Table 7 Statistical analysis of plant growth performance under different treatments

| Treatment  | Average height (cm) | Average fresh weight (g) | Average dry weight (g) | P-Value | Observation            |
|--|---------------------|--------------------------|------------------------|---------|------------------------|
| Control  | 30                  | 150                      | 30                     | —       | —                      |
| Dried mushroom powder + progesterone                     | 36                  | 180                      | 35                     | 0.05    | Significant difference |
| Dried mushroom powder (only)                             | 33                  | 160                      | 32                     | 0.10    | —                      |
| Calcinated dried mushroom powder (carbon) + progesterone | 39                  | 200                      | 40                     | 0.01    | Significant difference |
| Calcinated dried mushroom powder (carbon only)           | 36                  | 190                      | 38                     | 0.02    | Significant difference |



methodologies' sustainability and eco-friendliness must be assessed to evaluate how analytical techniques or procedures can affect the environment and the ecosystems. However, sustainability is a broad term that includes affordability, efficiency, safety, waste reduction, and greenness of the method. Greenness evaluation for the proposed method in this work is evaluated using the NEMI, AGP, and Modified GAPI (Mo GAPI) strategies that incorporate supportive approaches to enable a thorough evaluation from many perspectives.

**3.6.1. The NEMI greenness assessment method.** In 2002, NEMI was developed by the Methods and Data Comparability Board (MDCB).<sup>43</sup> It is one of the oldest GAC metrics. NEMI can be used as a searchable database. Its pictogram is a circle that has four parts, and each part represents a different criterion. The respective field of the NEMI pictogram is labeled with green color when the criterion value is met. If not, the corresponding part is uncolored. The first part of the NEMI label can be colored green with the requirement that the chemicals used in the corresponding analytical procedure are not present on the persistent, bioaccumulative, and toxic chemicals (PBT) list. The second part of the NEMI label can be marked with green if none of the solvents employed in the corresponding analytical procedures is hazardous and present on D, F, P, or U hazardous wastes lists. The third part of the NEMI label can be labeled with green color with the requirement that the pH of the sample is between 2 and 12. In this case, the corrosive effect on the environment can be avoided. The fourth part of the NEMI label can be marked with green color with the requirement that the amount of waste produced is no more than 50 g. NEMI has numerous merits as one of the oldest greenness metric systems.<sup>53</sup> NEMI is a simple GAC metric. Moreover, immediate and general information concerning the impacts of corresponding analytical procedures on the environment could be obtained just by a glance at the NEMI symbol (Fig. 8a).

**3.6.2. The AGP greenness assessment method.** NEMI was further improved as a new metric called AGP.<sup>54</sup> Compared to the original NEMI, the AGP is divided into five sections to assess the greenness of the analytical process with regard to safety, health, energy, waste, and the environment. Each section's green rating is determined by reference to National Fire Protection Association (NFPA) scores and specified dosage ranges, which are

visually represented on the pictogram using three different colors. The greenness of the above three different analytical assays is also evaluated by AGP. The results are shown in Fig. 8b.

**3.6.3. Modified GAPI greenness assessment method.** The total score in this MoGAPI assessment appears on the chart, and the color of the scale around the pentagrams indicates the overall evaluation of the method. The software used to calculate the score and to generate the MoGAPI assessment is freely available (open source) at [bit.ly/MoGAPI](http://bit.ly/MoGAPI). It should be noted that a similar modification has been recently applied to Complex-GAPI to assign a total score (90) as in Fig. 8c and an overall evaluation of analytical methods with pre-analytical procedures.<sup>55</sup>

**3.6.4. Greenness profile of eco-scale.** When performing their work, analytical chemists can take health, safety, and environmental concerns into account according to the concept of "green analytical chemistry" (GAC). If a technique's Eco-Scale score is higher than 75, it is deemed a superior green analysis. As the score gets closer to 100, the process will be more ecologically friendly. Because the new approach indicated a score of 94, it might be considered the epitome of a green method. Table 8 displays the score for the eco-scale.

**3.6.5. Greenness profile of AGREE.** A quick quantitative method that yields a score reflecting how well a methodology complies with the 12 key principles of green analytical chemistry is called AGREE, a green tool. Greener approaches are denoted by higher scores; the overall score is displayed in the centre of the circle pictogram, as shown in Fig. 9a.

Table 8 The penalty points (PPs) of the proposed method per the analytical eco-scale

|             | Analytical eco-scale | PPs |
|-------------|----------------------|-----|
| Reagents    | Ethanol              | 1   |
|             | Methanol             | 1   |
| Instruments | Oven                 | 2   |
|             | UV-Vis spectrometry  | 0   |
|             | X-ray diffractometry | 2   |
|             | Total pp             | 6   |
|             | Eco-scale            | 94  |

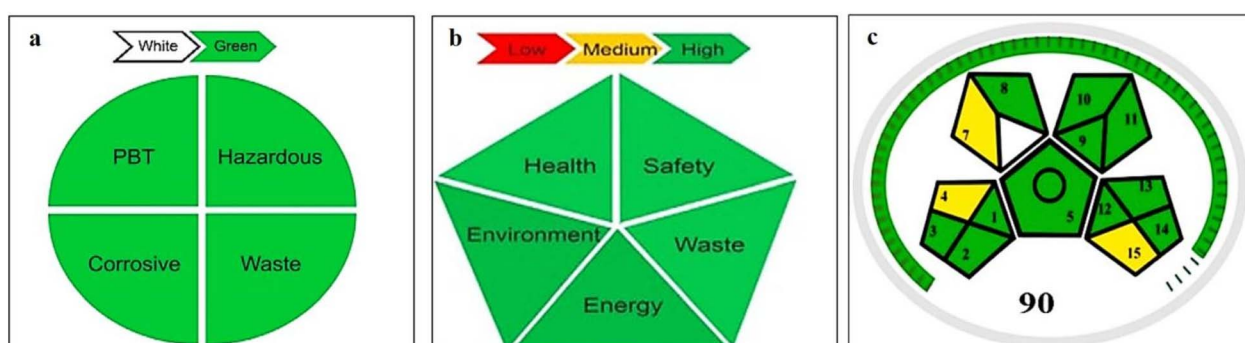


Fig. 8 (a) The pictogram of the NEMI gadget greenness tool, (b) the pictogram of the AGP gadget greenness tool, (c) the pictogram of modified GAPI gadget greenness tool.



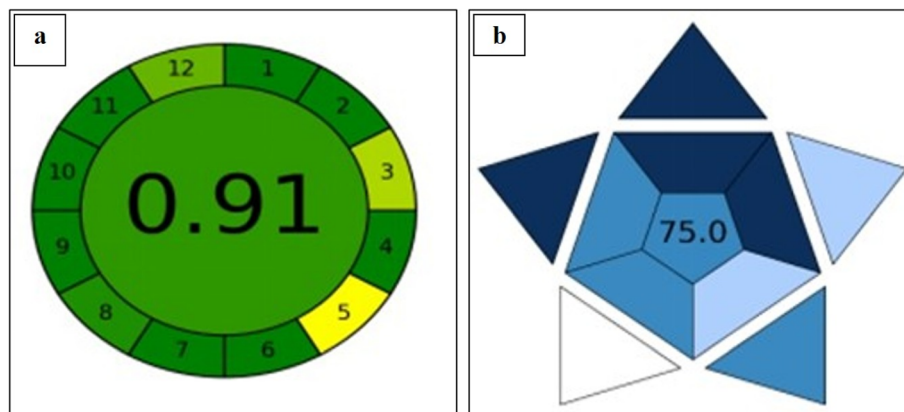


Fig. 9 (a) The score of the green metric AGREE for the new method, and (b) the BAGI blueness tool.

**3.6.6. Greenness profile of the BAGI blueness tool.** The composite BAGI index is computed using the approximate meaning of these scores. Ratings range from 1 (worst) to 10 (best) for each of these attributes. In our investigation, we employed the BAGI tool to evaluate the blueness of our proposed method. Our approach demonstrated its outstanding practical applicability, high production capabilities, automation possibilities, and exceptionally low operational costs by achieving an impressive BAGI score of 75, as illustrated in Fig. 9b.

### 3.7. Future perspectives and study limitations

However, this study presents a promising, eco-friendly approach for progesterone removal using reishi mushroom and its calcinated form, with significant potential for both environmental remediation and sustainable agriculture. Future research should focus on scaling up the process for industrial applications, integrating these adsorbents into existing water treatment systems, and conducting extensive field trials to validate their agricultural benefits. Optimizing adsorbent materials for enhanced capacity and selectivity, exploring regeneration methods, and extending their use to other endocrine-disrupting chemicals (EDCs) and soil remediation are critical next steps. Additionally, comprehensive life cycle and toxicity assessments are needed to evaluate environmental and health impacts. However, the study has limitations, including its reliance on controlled laboratory conditions, limited sample size, and short-term agricultural observations, which may not fully capture real-world variability or long-term effects. The complex adsorption mechanisms and economic viability of scaling up the process also require further investigation. Addressing these limitations while exploring broader applications will ensure the scalability, sustainability, and safety of this innovative technology, offering a holistic solution to water contamination and sustainable agriculture challenges.

## 4. Conclusion

This study successfully demonstrates the dual potential of reishi mushroom and its calcinated form as eco-friendly

adsorbents for progesterone removal and sustainable agricultural amendments. The optimized adsorption process, characterized by high efficiency, cost-effectiveness, and alignment with green chemistry principles, effectively addresses the challenge of endocrine-disrupting chemical (EDC) contamination in aquatic ecosystems. Furthermore, the integration of progesterone-adsorbed composites into agricultural systems significantly enhances plant growth, soil fertility, and crop productivity, showcasing a circular and sustainable approach to resource utilization. Molecular docking insights reveal the potential of ganoderic acid A and progesterone to modulate key plant hormone pathways, further supporting their role as growth enhancers. By bridging environmental remediation and agricultural innovation, this research offers a holistic solution to pressing global challenges, paving the way for future advancements in eco-sustainable technologies and promoting a greener, more sustainable future.

## Data availability

The authors declare that the data supporting the findings of this study are available within the article.

## Conflicts of interest

The authors declare no conflict of interest.

## Acknowledgements

This research has been funded by Scientific Research Deanship at University of Hail – Saudi Arabia through project number <<RG-24 148>>.

## References

- 1 E. R. Kabir, M. S. Rahman and I. Rahman, A Review on Endocrine Disruptors and Their Possible Impacts on Human Health, *Environ. Toxicol. Pharmacol.*, 2015, **40**, 241–258.

2 J. O. Tijani, O. O. Fatoba and L. F. Petrik, A Review of Pharmaceuticals and Endocrine-Disrupting Compounds: Sources, Effects, Removal, and Detections, *Water, Air, Soil Pollut.*, 2013, **224**, 1–29.

3 T. T. Schug, A. F. Johnson, L. S. Birnbaum, T. Colborn, L. J. Guillette Jr, D. P. Crews, T. Collins, A. M. Soto, F. S. Vom Saal and J. A. McLachlan, Minireview: Endocrine Disruptors: Past Lessons and Future Directions, *Mol. Endocrinol.*, 2016, **30**, 833–847.

4 T. K. Kasonga, M. A. A. Coetzee, I. Kamika, V. M. Ngole-Jeme and M. N. B. Momba, Endocrine-Disruptive Chemicals as Contaminants of Emerging Concern in Wastewater and Surface Water: A Review, *J. Environ. Manage.*, 2021, **277**, 111485.

5 Y. Chiang, S. T. Wei, P. Wang, P. Wu and C. Yu, Microbial Degradation of Steroid Sex Hormones: Implications for Environmental and Ecological Studies, *Microb. Biotechnol.*, 2020, **13**, 926–949.

6 A. Srivastava, B. Gupta, A. Majumder, A. K. Gupta and S. K. Nimborkar, A Comprehensive Review on the Synthesis, Performance, Modifications, and Regeneration of Activated Carbon for the Adsorptive Removal of Various Water Pollutants, *J. Environ. Chem. Eng.*, 2021, **9**, 106177.

7 Z. Jeirani, C. H. Niu and J. Soltan, Adsorption of Emerging Pollutants on Activated Carbon, *Rev. Chem. Eng.*, 2017, **33**, 491–522.

8 A. Hanif, H. N. Bhatti and M. A. Hanif, Removal of Zirconium from Aqueous Solution by *Ganoderma Lucidum*: Biosorption and Bioremediation Studies, *Desalin. Water Treat.*, 2015, **53**, 195–205.

9 S. Mooralitharan, Z. Mohd Hanafiah, T. S. B. Abd Manan, F. Muhammad-Sukki, WAAQI Wan-Mohtar and WHM Wan Mohtar, Vital Conditions to Remove Pollutants from Synthetic Wastewater Using Malaysian *Ganoderma Lucidum*, *Sustainability*, 2023, **15**, 3819.

10 L. Li, P. A. Quinlivan and D. R. U. Knappe, Effects of Activated Carbon Surface Chemistry and Pore Structure on the Adsorption of Organic Contaminants from Aqueous Solution, *Carbon*, 2002, **40**, 2085–2100.

11 H. Li, L. Chen, H. Chen, R. Xue, Y. Wang and J. Song, The Role of Plant Progesterone in Regulating Growth, Development, and Biotic/Abiotic Stress Responses, *Int. J. Mol. Sci.*, 2022, **23**, 10945.

12 S. Erdal and R. Dumluçinar, Progesterone and  $\beta$ -Estradiol Stimulate Seed Germination in Chickpea by Causing Important Changes in Biochemical Parameters, *Z. Naturforsch., C: J. Biosci.*, 2010, **65**, 239–244.

13 S. Sedaghathoor, S. K. A. Zare and A. Shirinpur-Valadi, Progesterone and Steroids In/On plants, *Progesterone-Basic Concepts Emerg. New Appl. Basic Concepts Emerg. New Appl.*, 2024, vol. 13.

14 D. S. Martins, B. R. Estevam, I. D. Perez, J. H. P. Américo-Pinheiro, W. D. Isique and R. F. Boina, Sludge from a Water Treatment Plant as an Adsorbent of Endocrine Disruptors, *J. Environ. Chem. Eng.*, 2022, **10**, 108090.

15 B. J. Chen, Y. Liu, B. C. Liu, R. B. Huang, P. L. Wu, T. Jiang, X. Dong, X. Li, H. E. Khoo and S. W. Lee, Chemical Modifications of Activated Carbons Prepared from Different *Ganoderma* Residues, Their Adsorption, and Catalytic Application, *Matéria*, 2024, **29**, e20230294.

16 A. Gałuszka, Z. Migaszewski and J. Namieśnik, The 12 Principles of Green Analytical Chemistry and the SIGNIFICANCE Mnemonic of Green Analytical Practices, *TrAC, Trends Anal. Chem.*, 2013, **50**, 78–84.

17 E. Y. Santali, I. A. Naguib, A. M. Alshehri, Y. A. Alzahrani, A. E. Alharthi, T. S. Alosaimi, B. D. Alsayali, I. Alsalahat, A. Almahri and M. A. S. Abourehab, Greenness Assessment of Chromatographic Methods Used for Analysis of Empagliflozin: A Comparative Study, *Separations*, 2022, **9**, 275.

18 J. Płotka-Wasylka, A New Tool for the Evaluation of the Analytical Procedure: Green Analytical Procedure Index, *Talanta*, 2018, **181**, 204–209.

19 F. Pena-Pereira, W. Wojnowski and M. Tobiszewski, AGREE - Analytical GREEnness Metric Approach and Software, *Anal. Chem.*, 2020, **92**, 10076–10082, DOI: [10.1021/ACS.ANALCHEM.0C01887/ASSET/IMAGES/LARGE/AC0C01887\\_0003.JPG](https://doi.org/10.1021/ACS.ANALCHEM.0C01887/ASSET/IMAGES/LARGE/AC0C01887_0003.JPG).

20 A. Gałuszka, Z. M. Migaszewski, P. Konieczka and J. Namieśnik, Analytical Eco-Scale for Assessing the Greenness of Analytical Procedures, *TrAC, Trends Anal. Chem.*, 2012, **37**, 61–72.

21 D. Maliwal, P. Jain, A. Jain and V. Patidar, Determination of Progesterone in Capsules by High-Performance Liquid Chromatography and UV- Spectrophotometry, *J. Young Pharm.*, 2009, **1**, 371, DOI: [10.4103/0975-1483.59330](https://doi.org/10.4103/0975-1483.59330).

22 A. Gürses, C. Doğar, M. Yalçın, M. Açıkyıldız, R. Bayrak and S. Karaca, The Adsorption Kinetics of the Cationic Dye, Methylene Blue, onto Clay, *J. Hazard. Mater.*, 2006, **131**, 217–228.

23 S. Senthilkumaar, P. R. Varadarajan, K. Porkodi and C. Subbhuraam, V Adsorption of Methylene Blue onto Jute Fiber Carbon: Kinetics and Equilibrium Studies, *J. Colloid Interface Sci.*, 2005, **284**, 78–82.

24 W. Rudzinski and W. Plazinski, Kinetics of Dyes Adsorption at the Solid– Solution Interfaces: A Theoretical Description Based on the Two-Step Kinetic Model, *Environ. Sci. Technol.*, 2008, **42**, 2470–2475.

25 M. Avrami, Kinetics of Phase Change. III: Granulation, Phase Change and Microstructure, *J. Chem. Phys.*, 1941, **9**, 177–184.

26 F. Ismail and S. Hassanen, Improvement of Egyptian Clover Yield and Quality by Using Bio and Organic Fertilizers in Newly Cultivated Saline Soil, *J. Soil Sci. Agric. Eng.*, 2019, **10**, 147–155.

27 Á. I. López-Lorente, F. Pena-Pereira, S. Pedersen-Bjergaard, V. G. Zuin, S. A. Ozkan and E. Psillakis, The Ten Principles of Green Sample Preparation, *TrAC, Trends Anal. Chem.*, 2022, **148**, 116530.

28 M. Sajid and J. Płotka-Wasylka, Green Analytical Chemistry Metrics: A Review, *Talanta*, 2022, **238**, 123046.

29 N. Manousi, W. Wojnowski, J. Płotka-Wasylka and V. Samanidou, Blue Applicability Grade Index (BAGI) and Software: A New Tool for the Evaluation of Method



Practicality, *Green Chem.*, 2023, **25**, 7598–7604, DOI: [10.1039/d3gc02347h](https://doi.org/10.1039/d3gc02347h).

30 L. Qian, C. Chen, Y. Lv, J. Li, X. Cao, H. Ren and M. L. Hassan, Preparation and Electrochemical Application of Porous Carbon Materials Derived from Extraction Residue of *Ganoderma Lucidum*, *Biomass Bioenergy*, 2022, **166**, 106593.

31 S. Sonal, P. Prakash, B. K. Mishra and G. C. Nayak, Synthesis, Characterization and Sorption Studies of a Zirconium (IV) Impregnated Highly Functionalized Mesoporous Activated Carbons, *RSC Adv.*, 2020, **10**, 13783–13798.

32 B. Sangeetha, A. S. Krishnamoorthy, D. Amirtham, D. J. S. Sharmila, P. Renukadevi and V. G. Malathi, FT-IR Spectroscopic Characteristics of *Ganoderma Lucidum* Secondary Metabolites, *J. Appl. Sci. Technol.*, 2019, **38**, 1–8.

33 S. P. Ospina Álvarez, D. A. Ramírez Cadavid, D. M. Escobar Sierra, C. P. Ossa Orozco, D. F. Rojas Vahos, P. Zapata Ocampo and L. Atehortúa, Comparison of Extraction Methods of Chitin from *Ganoderma Lucidum* Mushroom Obtained in Submerged Culture, *Biomed. Res. Int.*, 2014, **2014**, 169071.

34 S. M. Mousavi, S. A. Hashemi, A. Gholami, N. Omidifar, W.-H. Chiang, V. R. Neralla, K. Yousefi and M. Shokripour, *Ganoderma Lucidum* Methanolic Extract as a Potent Phytoconstituent: Characterization, in-Vitro Antimicrobial and Cytotoxic Activity, *Sci. Rep.*, 2023, **13**, 17326.

35 M. Fathi, M. Alami-Milani, M. H. Geranmayeh, J. Barar, H. Erfan-Niya and Y. Omidi, Dual Thermo-and PH-Sensitive Injectable Hydrogels of Chitosan/(Poly (N-Isopropylacrylamide-Co-Itaconic Acid)) for Doxorubicin Delivery in Breast Cancer, *Int. J. Biol. Macromol.*, 2019, **128**, 957–964.

36 F. J. Arévalo, P. G. Molina, M. A. Zón and H. Fernández, Studies about the Adsorption of Progesterone (P4) at Glassy Carbon Electrodes in Aqueous Buffer Solution by Square Wave Voltammetry, *J. Electroanal. Chem.*, 2009, **629**, 133–137, DOI: [10.1016/j.jelechem.2009.02.005](https://doi.org/10.1016/j.jelechem.2009.02.005).

37 C. Valenzuela-Calahorro, A. Navarrete-Guijosa, M. Stitou and E. M. A. Cuerda-Correa, Comparative Study of the Adsorption Equilibrium of Progesterone by a Carbon Black and a Commercial Activated Carbon, *Appl. Surf. Sci.*, 2007, **253**, 5274–5280, DOI: [10.1016/j.apsusc.2006.11.047](https://doi.org/10.1016/j.apsusc.2006.11.047).

38 J. M. McManus and N. Sharifi, Structure-Dependent Retention of Steroid Hormones by Common Laboratory Materials, *J. Steroid Biochem. Mol. Biol.*, 2020, **198**, 105572, DOI: [10.1016/j.jsbmb.2019.105572](https://doi.org/10.1016/j.jsbmb.2019.105572).

39 A. Wall, S. Björklund, A. P. S. Valetti and S. Shleev, *Optimizing Drug Delivery Predictability from Intravaginal Rings: the Role of Temperature and Surfactants* Nayab Hussain Supervisors, 2024.

40 Y. Liu, Is the Free Energy Change of Adsorption Correctly Calculated?, *J. Chem. Eng. Data*, 2009, **54**, 1981–1985, DOI: [10.1021/je800661q](https://doi.org/10.1021/je800661q).

41 D. M. Ruthven, *Principles of Adsorption and Adsorption Processes*, John Wiley & Sons, 1984, ISBN 0471866067.

42 A. Dąbrowski, Adsorption — from Theory to Practice, *Adv. Colloid Interface Sci.*, 2001, **93**, 135–224, DOI: [10.1016/S0001-8686\(00\)00082-8](https://doi.org/10.1016/S0001-8686(00)00082-8).

43 K. Y. Foo and B. H. Hameed, Insights into the Modeling of Adsorption Isotherm Systems, *Chem. Eng. J.*, 2010, **156**, 2–10, DOI: [10.1016/j.cej.2009.09.013](https://doi.org/10.1016/j.cej.2009.09.013).

44 B. J. Brownawell, H. Chen, J. M. Collier and J. C. Westall, Adsorption of Organic Cations to Natural Materials, *Environ. Sci. Technol.*, 1990, **24**, 1234–1241.

45 J. Perendija, V. Ljubić, M. Popović, D. Milošević, Z. Arsenijević, M. Đuriš, S. Kovač and S. Cvetković, Assessment of Waste Hop (*Humulus Lupulus*) Stems as a Biosorbent for the Removal of Malachite Green, Methylene Blue, and Crystal Violet from Aqueous Solution in Batch and Fixed-Bed Column Systems: Biosorption Process and Mechanism, *J. Mol. Liq.*, 2024, **394**, 123770, DOI: [10.1016/j.molliq.2023.123770](https://doi.org/10.1016/j.molliq.2023.123770).

46 D. Milošević, S. Lević, S. Lazarević, Z. Veličković, A. Marinković, R. Petrović and P. Petrović, Hybrid Material Based on Subgleba of Mosaic Puffball Mushroom (*Handkea Utriformis*) as an Adsorbent for Heavy Metal Removal from Aqueous Solutions, *J. Environ. Manage.*, 2021, **297**, 113358, DOI: [10.1016/j.jenvman.2021.113358](https://doi.org/10.1016/j.jenvman.2021.113358).

47 D. L. Milošević, N. Z. Tomić, V. R. Đokić, M. M. Vidović, Z. S. Veličković, R. Jančić-Heinemann and A. D. Marinković, Structural and Surface Modification of Highly Ordered Alumina for Enhanced Removal of Pb<sup>2+</sup>, Cd<sup>2+</sup> and Ni<sup>2+</sup> from Aqueous Solution, *Desalin. Water Treat.*, 2020, **178**, 220–239, DOI: [10.5004/dwt.2020.24982](https://doi.org/10.5004/dwt.2020.24982).

48 Y. Hu, P. E. Mortimer, K. D. Hyde, P. Kakumyan and N. Thongklang, Mushroom Cultivation for Soil Amendment and Bioremediation, *Circ. Agric. Syst.*, 2021, **1**, 1–14.

49 M. Iino, T. Nomura, Y. Tamaki, Y. Yamada, K. Yoneyama, Y. Takeuchi, M. Mori, T. Asami, T. Nakano and T. Yokota, Progesterone: Its Occurrence in Plants and Involvement in Plant Growth, *Phytochemistry*, 2007, **68**, 1664–1673.

50 A. K. Srivastava, Q.-S. Wu, S. M. Mousavi and D. Hota, Integrated Soil Fertility Management in Fruit Crops: An Overview, *Int. J. Fruit Sci.*, 2021, **21**, 413–439.

51 S. M. Mahgoub, M. R. Mahmoud, A. Y. Binsaleh, M. A. Almalki, M. A. Mohamed and H. F. Nassar, Analytical Assessment of a Novel RP-HPLC Method for the Concurrent Quantification of Selected Pharmaceutical Drugs Levodopa and Carbidopa Using Eight Greenness Metrics Comparing to the Lean Six Sigma Approach, *Sustainable Chem. Pharm.*, 2023, **36**, 101291.

52 H. M. Nassef, H. A. Ahmed, A. H. Bashal, M. A. El-Atawy, T. Y. A. Alanazi, S. M. Mahgoub and M. A. Mohamed, A Novel Six Sigma Approach and Eco-Friendly RP-HPLC Technique for Determination of Pimavanserin and Its Degraded Products: Application of Box-Behnken Design, *Rev. Anal. Chem.*, 2024, **43**, 20230073.

53 T. Y. A. Alanazi, M. A. Almalki, M. A. Mohamed and H. F. Nassar, Five Greenness Assessments of Novel RP-UPLC and MCR Methods for Concurrent Determination of Selected Pharmaceutical Drugs in Comparison with the



Lean Six Sigma Approach, *Microchem. J.*, 2023, **194**, 109359, DOI: [10.1016/j.microc.2023.109359](https://doi.org/10.1016/j.microc.2023.109359).

54 S. Armenta, F. A. Esteve-Turrillas, S. Garrigues and M. de la Guardia, Green Analytical Chemistry: The Role of Green Extraction Techniques, *Compr. Anal. Chem.*, 2017, **76**, 1–25.

55 F. R. Mansour, K. M. Omer and J. Plotka-Wasylka, A Total Scoring System and Software for Complex Modified GAPI (ComplexMoGAPI) Application in the Assessment of Method Greenness, *Green Anal. Chem.*, 2024, **10**, 100126.

